Urban Surface Radiative Energy Budgets Determined Using Aircraft Scanner Data

Jeffrey C. Luvall[1] jluvall@msfc.nasa.gov, (256) 961 7886, Dale A. Quattrochi[1], Doug L. Rickman[1] and Maury G. Estes[2]
[1]NASA Global Hydrology and Climate Center, Marshall Space Flight Center
[2]Universities Space Research Association

Introduction

One of the earliest recognized and measured phenomena of urbanization is the urban heat island (UHI) which was reported as early as 1833 for London and 1862 for Paris. The urban heat island results from the energy that is absorbed by man-made materials during the day and is released at night resulting in the heating of the air within the urban area. The magnitude of the temperature difference is highly dependent on the structure of the urban area, amount of solar insolation, and atmospheric conditions during the night. These air temperature differences may be as large as 10° F greater than the surrounding countryside. This phenomena is not limited to large urban areas, but also occurs in smaller metropolitan areas. The UHI has significant impacts on the urban air quality, meteorology, energy use, and human health.

Although satellite data are very useful for analysis of the urban heat island effect at a coarse scale, they do not lend themselves to developing a better understanding of which surfaces across the city contribute or drive the development of the urban heat island effect. Analysis of thermal energy responses and energy budgets for specific or discrete surfaces typical of the urban landscape (e.g., asphalt, building rooftops, vegetation) requires measurements at a very fine spatial scale (i.e., < 15m) to adequately resolve these surfaces and their attendant thermal energy regimes. Additionally, very fine scale spatial resolution thermal infrared data, such as that obtained from aircraft, are very useful for demonstrating to planning officials, policy makers, and the general populace the benefits of planning cool communities. These benefits include mitigating the urban heat island effect, making cities more aesthetically pleasing and more habitable environments, and sustainable communities.

High spatial resolution visible and thermal data are required to quantify how artificial surfaces within the city contribute to an increase in urban heating and the benefit of cool surfaces (e.g., surface coatings that reflect much of the incoming solar radiation as opposed to absorbing it thereby lowering urban temperatures.

Measures to mitigate the urban heat island include afforestation and the widespread use of highly reflective surfaces.

Methods

Surface Energy and Radiation Budget

Surface temperature is a major component of the surface energy budget. Knowledge of it is important in any attempt to describe the radiative and mass fluxes which occur at the surface. Use of energy terms in modeling surface energy budgets allows the direct comparison of various land surfaces encountered in a landscape, from vegetated (forest and herbaceous) to non-vegetated (bare soil, roads, and buildings) (Oke, 1987). The partitioning of energy budget terms depends on the surface type. In natural landscapes, the partitioning is dependent on canopy biomass, leaf area index, aerodynamic roughness, and moisture status, all of which are influenced by the development stage of the ecosystem.. In urban landscapes, coverage by man-made materials substantially alters the surface energy budget.

The net all-wave radiation balance (Wm^{-2}) of landscape canopies can be determined following Oke, 1987.

Net solar radiation, K^*
, is given by

$$K^* = (1-\alpha)(K\downarrow)$$

(1)

where:

α = site albedo

$K\downarrow$ = incoming solar radiation

Albedo is defined as:

$$\alpha = \frac{K\uparrow}{K\downarrow} \qquad (2)$$

where:

$K\uparrow$ = reflected solar radiation

The long wave energy emitted from a surface ($L\uparrow$) is dependent on surface temperature:

$$L\uparrow = \varepsilon[\sigma T^4] \qquad (3)$$

where:

ε = emissivity

σ = Stefan-Boltzman constant (5.7 x 10^{-8} $\mathrm{Wm^{-2}}$ $\mathrm{K^{-4}}$)

T = land surface temperature (Kelvin)

The net long wave radiation at the surface, L^* is given by

$$L^* = L\downarrow - L\uparrow \qquad (4)$$

where:

$L\downarrow$ = long wave radiation from the atmosphere

Therefore, the net all-wave radiation, Q^*, can be given as:

$$Q^* = K^* + L^* \qquad (5)$$

Net radiation is a particularly useful term because, under most conditions, it represents the total amount of energy available to the land surface for partitioning into non-radiative processes (mass heating, biological synthesis, etc.) at the surface. It is the amount of energy the system holds on to and degrades. In vegetated areas the amount of net radiation is dependent upon vegetation type and varies with canopy leaf area and structure.

Net radiation may be expressed as the sum of these non-radiative fluxes:

$$Q^* = \lambda E + H + G \qquad (6)$$

where:

H = the sensible heat flux

λ = the latent heat of vaporization of water

E = transpiration flux

G = energy flux into or out of storage (both canopy & soil)

The partitioning of λE, H, and G are also dependent on the makeup of the surface. Both the physiological control of moisture loss (stomatal resistance) and leaf/canopy morphology for vegetation determines how Q^* is partitioned among λE, H, and G. For urban surfaces the coverage of both man-made materials and vegetation results in a heterogeneous mixture of surfaces which determine the partitioning of energy.

The remotely sensed data obtained from the ATLAS (see below) allows the measurement of important terms in the radiative surface energy budget: $K\downarrow$ and $L\uparrow$ on a urban landscape scale. When combined with output from MODTRAN4 (Berk et al. 1999) atmospheric radiance models the remaining terms $K\uparrow$ and Q^* can be determined.

The change in surface temperature as a function of time is an additional property that can be measured using ATLAS data. . This may be done using repeated over flights. Usually a separation of about 30 minutes results in a measurable change in surface temperature caused by the change in incoming solar radiation. Their ratio can be used to define a surface property defined by Luvall and Holbo (1989) as a Thermal Response Number $(KJ\,m^{-2}\,{}^{o}C^{-1})$.

$$\text{TRN} = \frac{\int_{t1}^{t2} [(Q^*)(\Delta t)]}{\Delta T} \qquad (7)$$

Where Q^* is total net radiation and ΔT change in surface temperature for time period t_1 to t_2.

The TRN provides an analytical framework for studying the effects of surface thermal response for large spatial resolution map scales that can be aggregated for input to smaller-scales, as needed by climate models. The importance of TRN is that: 1. it is a functional classifier of land cover types; 2. it provides a initial surface characterization for input to various climate models; 3. it is a physically based measurement; 4. it can be determined completely from remotely sensed data; and 5. it is a scale independent measurement that can be examined from a pixel by pixel measurement or by extracting a polygon from the landscape feature containing multiples of pixels representing the required element. The TRN can be used as an aggregate expression of both surface properties (forest canopy structure and biomass, age, and physiological condition; urban structures and material types) and environmental energy fluxes

ATLAS data collection

ATLAS is a 15-channel sensor that incorporates the bandwidth range of the Landsat Thematic Mapper (TM) with additional bands in the middle reflective infrared and thermal IR range (Figs. 1 & 2).

The ATLAS can collect data ranging from 2 to 20 meters in resolution. All of the channels have onboard calibration, which permits verification of radiometry on an ongoing basis. Visible channel calibration is provided by a onboard integrating sphere. Thermal channel calibration is provided by onboard blackbodies. All calibration data is written to the house keeping areas of the data file for use in data calibration. Aircraft positioning information is recorded in housekeeping areas through the use of a onboard GPS system and dedicated gyroscopes. The ATLAS sensor is particularly attractive to our study for several reasons. All bands share the sample spatial resolution. This permits direct comparison of radiometry across all channels. The ATLAS also has superior spectral resolution within the thermal IR channels. These offer the potential to make accurate measurements of thermal responses for different landscape characteristics and their corresponding land-atmosphere interactions over small wavelength regions. The ATLAS is operated by the NASA Stennis Space Center and is flown onboard a Lear 23 jet aircraft.

ATLAS data were collected over each of the pilot cities, Baton Rouge, Sacramento, and Salt Lake City during 1998. For each city, approximately a 30 by 30 mile area was covered by north-south flight lines.

Flights were flown within about 3 hours of solar noon on May 11 for Baton Rouge, June 29 for Sacramento, and September 15 for Salt Lake City. All data were collected at 10 m resolution.

Atmospheric correction and ATLAS data calibration

The measurement and modeling of the atmospheric correction needed to produce calibrated data sets from ATLAS is an extremely complex procedure. It requires direct measurements of the atmosphere extension coefficients by wavelength and profiles of atmospheric temperatures and water vapor. ATLAS instrument characteristics and calibration are also required. Fig. 3 details the process flow followed for this project. A combination of software was used for the processing, including the public domain image processing/remote sensing package ELAS (Beverley and Penton, 1989; Graham et al 1986) and a series of custom programs. MODTRAN4 (Berk et al. 1999) was used to model the atmospheric radiance and transmittance using input from radiosonde data and shadow band radiometers.

Rickman et. al (2000) procedure for calibrating the ATLAS sensor to produce the system transfer function to convert digital values (DV) into radiance measurements. These procedures produce ATLAS data files that are in physical units of energy. These files are used for the generation of files which derive albedo (channel 1) surface temperature (channel 2).

Results and Discussion

ATLAS data were collected during clear sky conditions thus eliminating the problems with clouds shading the surface. These conditions provided uniform energy loading for the entire flight area. Incoming solar radiation fluxes for Baton Rouge and Sacramento were generally over 1000 wm^{-2}. Since Salt Lake City was flown later in the year, incoming solar radiation was lower, about 900-1000 wm^{-2} . Long wave radiation fluxes for all cities averaged around 320 to 380 wm^{-2} .

The corresponding albedo and surface temperature measurements from the mosaic produced from the flight lines for each city (Table 1.) indicated that Salt Lake City had the overall highest average albedo followed by Baton Rouge and then Sacramento. However, even though Salt Lake City had the greatest albedo and the lowest solar loading, it was the warmest city, with average surface temperatures 4.8 oC warmer than the coolest city, Sacramento.

Table 1. Average albedo and surface temperatures derived from ATLAS mosaic data

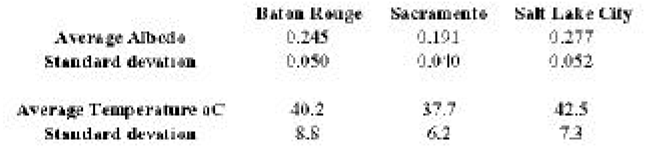

	Baton Rouge	Sacramento	Salt Lake City
Average Albedo	0.245	0.191	0.277
Standard deviation	0.050	0.040	0.052
Average Temperature oC	40.2	37.7	42.5
Standard deviation	8.8	6.2	7.3

Its important to understand why Salt Lake City is warmer even though its albedo was higher, since one of the urban heat island mitigation strategies is to increase the city's albedo to reduce warming. One must examine how the sun's energy is partitioned once its received by the surface. Equation 6 shows that here are only three pathways the energy from net radiation can take:
1. evaporate water (latent heat); 2. warm the air (sensible heat); and 3. ground (storage). Even though a surface may have a higher albedo, if that surface is not partitioning the energy into latent heat, it is going to warm up. This is a good example of how one must understand the surface energy budget in order to make intelligent decisions when incorporating the urban heat island mitigation strategies to both urban heating and air quality issues.

A mosaic of the measured albedo for Baton Rouge is seen in Fig. 4. The impact of urbanization on the albedo value in comparison to the surrounding countryside can readily be examined. The river and wetlands had the lowest albedo, followed by forested areas. The urbanized areas had the highest albedo. A good way to examine the albedo structure is to produce a frequency graph of occurrence of the albedo value of each pixel. The shape of the frequency graph shows the albedo structure of Baton Rouge (Fig. 5). The river readily shows up as a peak in the low albedo values. There are very few areas of high albedo. This is significant, since EPA's Energy Star roofs are required to have an albedo

0.67.

In the surface temperature mosaic for Baton Rouge, the urbanized areas can easily be identified (Fig. 6). The river and vegetated areas are the coolest with the roofs and paved areas the warmest. The shopping mall to the east is identified by its hot roofs and parking lot, along with the refinery on the east side of the Mississippi River.

The temperature frequency distribution for Baton Rouge (Fig. 7) readily identifies important land surface features that make up the thermal fabric of the city. First, the Mississippi River is identifiable by its peak as the coolest surface. The next coolest peak identifies the vegetated component. The hottest surfaces correlates with roofs and asphalt pavements and is represented by the "tail" of the distribution.

It is useful to compare the albedo and thermal values among the three cities. (Tables 2 & 3). The range of albedo of 0.20-0.30 encompassed about 82 % of the surface area in Sacramento, but only 57 % for Baton Rouge and 64 % for Salt Lake City. If the 0.35 albedo range is included, then the differences among the cities are reduced. The albedo range for 0.20 to 0.35 accounts for the majority of the surface albedo values, in Baton Rouge about 91 %, Sacramento 90 % and Salt Lake City 90 %. There was also a significant difference among the cities in the amount of surface with an albedo of > 0.50. Baton Rouge 0.041% and Sacramento, 0.039 were also most identical, however Salt Lake City at 0.50%, was much greater.

A majority of the temperatures fell within the range of 30-45 ^{o} C. In Baton Rouge and Salt Lake City about 72% of the surface temperatures fell within that range, in Sacramento it was greater at 90 %. The most significant difference was for the hotter temperatures above 50 ^{o} C, where both Salt Lake City 27.1 %, and Baton Rouge 23% were similar, but Sacramento 5.5% was much lower. The values of albedo and temperature given these tables illustrate how different each city is in terms of their "urban fabric".

The main technique for "classification" of urban land surfaces is to examine using land use or by surface type, ie roof, road, vegetated, etc. and assign a albedo or temperature to that class. These "classes" are then input into some meteorological or air quality model. It is important to point out that traditional image classification techniques use only differentiation of surfaces in the visible wave lengths and not functional differentiation, i.e. how the surface functions in some respect. In a typical classification approach a key assumption is that the albedo gives a indication of how that surface may partition the sun's energy. This is a false assumption because the way each surface partitions energy is unique depending on material type, vegetated or non-vegetated, water status, atmospheric vapor deficits, and the relative mixtures and arrangements of the various components of that surface. The albedo is only one part of determining what the surface temperature will be and how the surface partitions energy (eqs. 5 & 6) What is needed is a functional classification of surface types in an urban area based on how that surface partitions Q*. The Thermal Response Number (TRN) and surface temperatures provide key elements to such a functional classification. Table 4 allows the comparison among the cities for albedo, net radiation, surface temperature, change in surface temperature over time and the TRN for four different land use types. Generally the industrial areas had the highest albedo, and the hottest temperatures. The park areas the lower albedo (not always the lowest) and lowest temperatures. The partitioning of Q* can be evaluated using the TRN. The greater the TRN the more energy is being used to evaporate water rather than to heat the air. For example, the Park in Baton Rouge has a TRN of 5903 kJ m $^{-2}$ ^{o}C^{-1} and a small 👎T over the measurement period. In other areas the 👎T is much greater and the TRN is smaller. In Salt Lake City the park TRN is only 299 kJ m $^{-2}$ ^{o}C^{-1}

compared to 701 kJ m^{-2} ^{o}C^{-1} for the park in Sacramento and ☟T of 4.1 ^{o}C and 2.2 ^{o} C, indicating that less of the surface energy is being partitioned into latent heat flux and more into heating the air. It appears that the trees in the Salt Lake City park were not transpiring (latent heat flux) as much as the Baton Rouge or Sacramento trees. Luvall (1997) found for a white pine canopy a TRN of 1053 at midday and tower based measurements of latent heat fluxes of 411 Wm^{-2} .

Since albedo alone does not truly reflect how the lands' surface partitions energy, one needs additional information to asses the "urban fabric" of the city. Including surface temperature provides the needed additional information. The ATLAS data sets provide the needed calibrated and quantifiable data sets in physical units. Since we are working in physical units, the TRN, surface temperature and albedo classifications represents a functional classification of that surface, that can readily incorporated into the surface parameterization of meteorological and air quality models.

Each city as illustrated by Baton Rouge has a distinctive "energy print" that is characteristic of the surface composition and how its processing energy (Fig 8). For example the rivers, ie dark and cool, show up quite nicely in Baton Rouge and Sacramento as the lower left corner of the skattergram. These scattergams become a very powerful classification tool representing the functional classification of urban land surfaces (Figs. 9, 10, 11). Within each city, each land use has a unique "energy print" that is directly physically related to how that surface is processing energy. These "energy prints" of the land use are unique for each city; ie, the Sacramento CBD (Central Business District) skattergram is significantly different than Baton Rouge or Salt Lake City's CBD skattergram. These results again empathize that classifications based on cover type/land use cannot be applied across a variety of cities, since they cannot represent the true energy partitioning of that surface.

Conclusions

The urban landscape represents a complex heterogeneous surface that strongly influences the development of the urban heat island. The urban landscape cannot adequately classified using traditional structural based remote sensing classification techniques because these techniques are not directly related to the physical functioning of the surface energy budget. Calibrated and atmospherically corrected ATLAS data sets are required to quantify the surface energy budget. These data need to be incorporated into both meteorological and air quality models in order to assess the effectiveness of the heat island mitigation strategies. This study also proved that each city was unique in its albedo and surface temperature characteristics. It also demonstrates the importance of vegetation in keeping the city cool.

References

Anderson, J. E.; 1992; Determination of Water Surface Temperature Based on the Use of Thermal Infrared Multispectral Scanner Data; Geocarto International, pp 3-8.

Berk, A, G.P. Anderson, P.K. Acharya, J.H. Chetwynd, L.S. Bernstein, E.P. Shettle, M.W. Matthew, and S.M. Adler-Golden, 1999. MODTRAN4 Users Manual. Air Force Research Laboratory, Space Vehicles Directorate, Air Force Material Command, Anscom AFB, MA 01731-3010.

Beverley, A.M., and Penton, P.G.; 1989; ELAS, Earth Resources Laboratory Applications Software Vol II, User Reference; Earth Resources Lab. Report No. 183; NSTL, Mississippi.

Graham, M.H., Junkin, B.G., Kalcic, M.T., Pearson, R.W. and Seyfarth, B.R.. 1986. ELAS - Earth Resources Laboratory Applications Software. Revised Jan 1986, NASA/NSTL/ERL Report No. 183.

Luvall, J.C. and Holbo, H.R. 1989. Measurements of short-term thermal responses of coniferous forest canopies using thermal scanner data. Remote Sensing of Environment 27:1-10.

Luvall, J.C. 1997. The use of remotely sensed surface temperatures from an aircraft-based Thermal Infrared Multispectral Scanner (TIMS) to estimate the spatial and temporal variability of latent heat fluxes and thermal response numbers from a white pine (*Pinus strobus L.*) plantation. *In* Scale in Remote Sensing and GIS. pp. 169-185. Edited by D.A. Quattrochi and M.F. Goodchild. CRC/Lewis Publishers, Boca Raton, Florida.

Oke, T. R., 1987. Boundary Layer Climates. John Wiley & Sons, New York, 372 pp.

Rickman, D.L.; J. C. Luvall, and S. Schiller. In press. An algorithm to atmospherically correct visible and thermal airborne imagery. Workshop on Multi/Hyperspectral Technology and Applications, Redstone Arsenal, Alabama.